Pure & Appl. Chem., Vol. 71, No. 2, pp. 321–335, 1999.
Printed in Great Britain.

INTERNATIONAL UNION OF PURE AND APPLIED CHEMISTRY

ORGANIC CHEMISTRY DIVISION COMMISSION ON PHOTOCHEMISTRY*

TERMINOLOGY, RELATIVE PHOTONIC EFFICIENCIES AND QUANTUM YIELDS IN HETEROGENEOUS PHOTOCATALYSIS. PART II: EXPERIMENTAL DETERMINATION OF QUANTUM YIELDS†

(Technical report)

Prepared for publication by
ANGELA SALINARO,[1] ALEXEI V. EMELINE,[1] JINCAI ZHAO,[2] HISAO HIDAKA,[3] VLADIMIR K. RYABCHUK,[4] AND NICK SERPONE[1]

[1] Department of Chemistry & Biochemistry, Concordia University,1455 deMaisonneuve Blvd. West, Montreal (Quebec) Canada H3G 1M8.
[2] Institute of Photographic Chemistry, Chinese Academy of Sciences, Beijing 100101, China.
[3] Department of Chemistry, Meisei University, 2-1-1 Hodokubo, Hino, Tokyo 191, Japan.
[4] Department of Physics, University of St. Petersburg, Ulianovskaia St. 1, St. Petersburg, Russia 198904.

*Membership of the Commission 1996–98 during which this Report was prepared was as follows:

Chairman: Prof. J. R. Bolton (Canada, 1996–99); *Secretary*: Prof. R. G. Weiss (USA, 1998–99); *Titular Members*: Prof. J. R. Bolton (Canada); Prof. R. G. Weiss (USA); Prof. H. Bouas-Laurent (France); Prof. J. Wirz (Switzerland); *Associate Members*: Dr A. U. Acuña Fernandez (Spain), Prof. H. Dürr (Germany), Prof. H. Masuhara (Japan), Prof. N. Serpone (Canada); *National Representatives*: Prof. C. Wentrup (Australia), Dr V. G. Toscano (Brazil), Prof. F. C. de Schryver (Belgium), Prof. C. H. Tung (Chinese Chemical Society), Dr G. Pandey (India), Prof. I. Willner (Israel), Prof. S. C. Shim (Korea), Prof. S. J. Formosinho Sanches Simões (Portugal), Dr P. Hrdlovic (Slovakia).

†A draft version of this paper was published previously in part in [*J. Photochem. Photobiol. A:Chem.*, *J. Adv. Oxid. Technol.*; *IAPS Newsletter* and *EPA Newsletter*] to solicit comments and critiques from the scientific and engineering community. Moreover, during the preparation the draft proposal was submitted to a number of distinguished photochemists and photocatalycists to get their views.

Relative photonic efficiencies and quantum yields in heterogeneous photocatalysis. Part II: Experimental determination of quantum yields (Technical Report)

Abstract: In the preceding article [*Pure Appl. Chem.* **71**, 303–320 (1999)] we examined two principal features of heterogeneous photocatalysis that demanded scrutiny: (i) description of photocatalysis and (ii) description of process efficiencies. For the latter we proposed a protocol *relative photonic efficiency* which could subsequently be converted to quantum yields. A difficulty in expressing a quantum yield in heterogeneous photochemistry is the very nature of the system, either solid/liquid or solid/gas, which places severe restrictions on measurement of the photon flow absorbed by the light harvesting component, herein the photocatalyst TiO_2, owing to non-negligible scattering by the particulates. It was imperative therefore to examine the extent of this problem. Extinction and absorption spectra of TiO_2 dispersions were determined at low titania loadings by normal absorption spectroscopy and by an integrated sphere method, respectively, to assess the extent of light scattering. The method is compared to the one reported by Grela *et al*. [*J. Phys. Chem.* **100,** 16 940 (1996)] who used a polynomial extrapolation of the light scattered in the visible region into the UV region where TiO_2 absorbs significantly. This extrapolation underestimates the scattering component present in the extinction spectra, and will no doubt affect the accuracy of the quantum yield data. Further, we report additional details in assessing limiting photonic efficiencies and quantum yields in heterogeneous photocatalysis.

INTRODUCTION

Heterogeneous photocatalysis has had its usefulness explored as a viable alternative technology to classical 'best' technologies in both environmental detoxification [1–9] and in energy conversion devices [10]. This technology has witnessed significant advances during the last decade, and is actively being exploited towards the photooxidative mineralization of harmful environmental organic substrates (e.g. pesticides, herbicides, and others) by the utilization of illuminated semiconductor photocatalysts, amongst which anatase TiO_2 predominates.

Acting as pools of electrons and holes, photoexcited TiO_2 particulates can be capitalized on in redox reactions. The scheme below summarizes but a fraction of the several events/processes that can ensue following illumination of this semiconductor at the bandgap energy $E_g = 3.2$ eV or higher (wavelengths below $\approx$385 nm) (Scheme 1), where subsequent to their formation conduction band electrons and valence band holes are trapped by lattice defects or as Ti^{3+} (trapped electron) and as $Ti^{IV}–O^{-\cdot}–Ti^{IV}$ (trapped hole), recombine in the bulk and/or migrate to the surface in short time (few ps) where they may also be trapped by surface defects or trapped by adsorbed species such as O_2 for the electron to give the superoxide radical anion, $O_2^{-\cdot}$, and by surface OH^- (or H_2O) for the hole to yield a surface-bound $^{\cdot}OH$ radical, $\equiv Ti–{}^{\cdot}OH$ [11]. Ultimately, these surface trapped carriers react with organic substrates RH to give photooxidized intermediates and ultimately carbon dioxide; reducible species such as metal ions form metal deposits. Additional steps/processes can be envisaged some of which have been corroborated, e.g. formation of organic peroxides [12], or inferred, e.g. formation of tetraoxides ROOOOH [4]. Conference proceedings [7], monographs [8] and review articles [1–6,9,13] have been published that summarize much of our recent knowledge of this exciting novel technology: heterogeneous photocatalysis.

An issue of significant debate in this area has been the expression of process efficiency for the light-driven conversion of an organic substrate RH to its ultimate mineralization. The goal is to assess process quantum yield, Φ_λ, as described in homogeneous photochemistry {see Part I of this series [14]}.

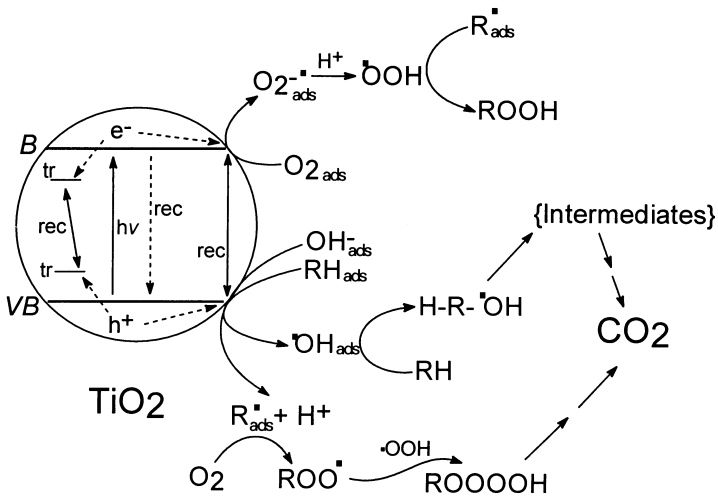

Scheme 1

Unfortunately, the presence of a heterogeneous (e.g. solid/liquid) phase has limited our ability to determine the exact number (or photon flow, $R_{o,\lambda}$) of photons absorbed by the solid phase, since the extent of light scattered by the metal-oxide (e.g. TiO_2) photocatalyst is not insignificant. According to a recent report, the extent of scattering can vary from 13% to 76%, depending on conditions, of the total incident photon flow; variation in pH of the suspension also appears to influence the extent of scattering [15]. As well, Cabrera *et al*. [16] noted that only ≈15% (Aldrich TiO_2) of the radiation measured by homogeneous actinometry inside a reactor was effectively absorbed. Possible solutions to assess the fraction of light absorbed in a heterogeneous photocatalytic process have been proposed [15–20]. A simple protocol to assess process efficiencies was proposed in Part I [14], and referred to as *relative photonic efficiency*, ξ_r. Subsequently values of ξ_r can be converted to quantum yields.

The efficiencies ξ_r reported elsewhere [17] and reproduced earlier (cf. tables 1 and 2 of Part I [14]) referred specifically to substrate disappearance and demonstrated the general applicability of the proposed protocol. Although the ξ_r are those for substituted phenols, the concept of relative photonic efficiency is not restricted to these species; it can also be applied to other aromatic substances with phenol as the standard substrate against which all ξ_r are reported. The effects of variations in light irradiance, reactor geometry, pH, temperature, concentration of organic substrate, and loading of photocatalyst material TiO_2 on the ξ_r data have also been examined [17] for 2-methylphenol, 2,4-dimethylphenol, and 4-chlorophenol (Fig. 1) as well as for other organic substrates.

The effects of the nature and the source of various TiO_2 specimens on ξ_r were also explored [17]. The Tioxide, Sargent-Welch and Fluka titania specimens were twice more efficient than the Degussa P-25 TiO_2 specimen at least for the initial photooxidation of phenol. Spin-trap EPR studies have demonstrated that production of $^{\bullet}OH$ radicals on Degussa P-25 TiO_2 (≈ 80% anatase, 20% rutile) relative to those generated on an Aldrich (100% anatase) sample differed by a factor of ≈1.9 [21] inferring the Degussa P-25 TiO_2 to be more efficient towards photooxidations by such radicals.

In assessing the quantum yield of a photochemical, photophysical, or photocatalytic process there is the requirement that the actual number of photons, n_{ph}, or photon flow, $R_{o,\lambda}$, from the radiation source absorbed by the substrate or photocatalyst in a heterogeneous system be known. To evaluate the fraction of light absorbed necessitates that the absorption spectrum of the light harvester or photocatalyst also be known. In a heterogeneous system such as solid/liquid, scattering effects impinge strongly on the absorption spectrum; what is typically measured in such a system is the extinction spectrum. Brief consideration suggests that determination of the true absorption spectrum of polydispersed titania particles suspended in an aqueous medium is best carried out by a spectrophotometric integrating sphere technique which will account for the photons scattered, transmitted and absorbed. This method has recently been applied successfully [18,19].

Grela and co-workers [20] reported an empirical simple method to estimate the extent of scattering at

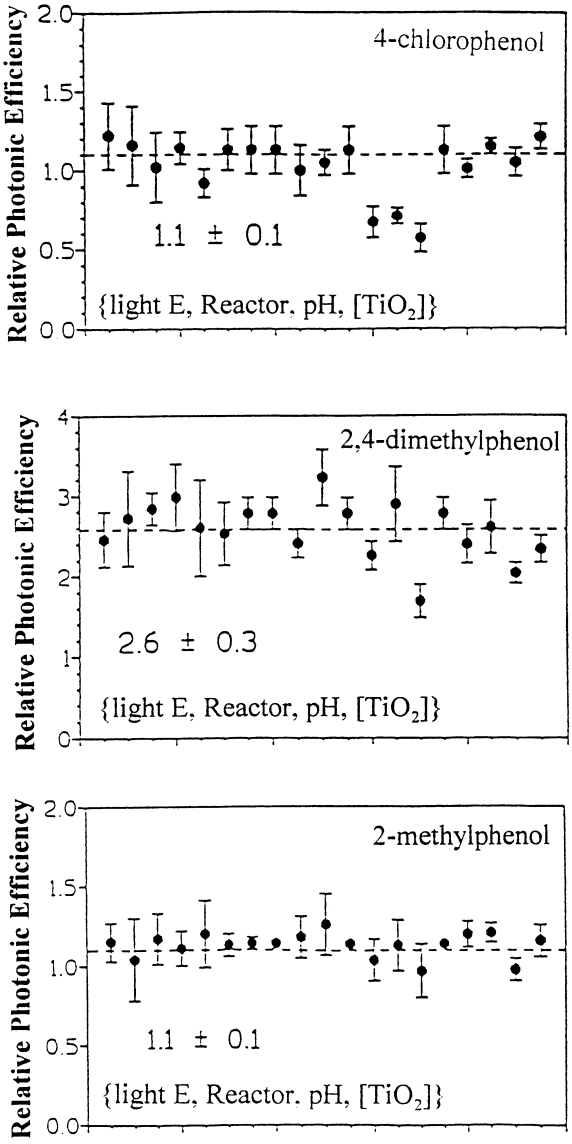

Fig. 1 Relative photonic efficiencies for 4-chlorophenol, 2,4-dimethylphenol and 2-methylphenol showing the values used to calculate averages; includes only the effects of light intensity, reactor geometry, pH and concentration of titania; $[\text{substrate}]_i \approx 20$ mg/L.

295 nm in a thin slab of polydispersed illuminated TiO_2 solution to assess the **approximate** *quantum yield* for the initial formation of the DMPO-$^{\cdot}$OH spin adduct. The baseline at wavelengths between 400 and 550 nm in the extinction spectrum of the solution was extrapolated to 250 nm by a quadratic extrapolation method, rather than by the theoretical λ^{-4} dependence that typically describes light scattering by particles. No reasons were given for the choice of a quadratic extrapolation method. The absorbance of the TiO_2 colloidal solution examined and corrected for residual scattering at 295 nm was $\approx$70% of the extinction spectrum determined by normal absorption spectroscopy [20].The discrepancy between this study and the methods used by others [15,16], together with the rather empirical and simplistic approach of [20], especially since the conditions of the suspensions can affect the proportion of light scattered, led us to examine the degree to which titania particles scatter incident light radiation.

During the course of our work [19] to systematize a protocol and methodology to determine quantum yields in heterogeneous photochemistry, we measured the absorbance of Degussa P-25 TiO_2 (the same as used by Grela *et al*. [20]) and of a sample of the Hombikat UV-100 TiO_2 by the integrating sphere method employing the procedures reported elsewhere [18,19]. We compare the integrating sphere method with

the empirical method used by others [20] to test the validity of the latter. We find that the empirical method significantly underestimates the extent of scattering below ≈380 nm. The scattering tends to plateau below ≈340 nm in the region where the Degussa P-25 TiO_2 absorbs significantly. We also report some experimental details in the protocol used to estimate relative photonic efficiencies and quantum yields.

EXPERIMENTAL

Materials

The Degussa P-25 TiO_2 specimen was a gift from Degussa Canada Ltd. and the Hombikat UV-100 titania sample was obtained from Sachtleben Chemie GmbH (Duisburg, Germany). The phenol and the 4-chlorophenol were available from earlier studies.

Degussa P-25 TiO_2 consists of two crystalline phases ≈80% anatase and ≈20% rutile and contains traces of SiO_2, Al_2O_3, HCl and Fe; it is a nonporous solid with a BET specific surface area of ≈55 m^2/g and its crystallites range between 25 and 35 nm [22].These crystallites aggregate in a regular dispersion; sizes vary between 50 nm and 200 nm [23,24]. The Hombikat UV-100 TiO_2 is 100% anatase with particle size less than 10 nm and with a BET specific surface area of ≈186 m^2/g [25].

The polydispersed titania solutions were obtained by sonication/centrifugation procedures reported elsewhere [18–20]. To prepare the colloidal solutions, a 250-mL acidifed (0.01 M HCl) aqueous suspension of 2 g/L in Degussa P-25 TiO_2 was sonicated with an ultrasonic 250-Watt cell disrupter (Sonics & Materials) at a power of ≈50 W for 15 min; the milky dispersion was then centrifuged (2000 r.p.m.) in 50-mL portions until a transparent colloidal solution was obtained. This solution was extracted and left to evaporate slowly at ambient temperature. Approximately 250 mg of the TiO_2 was recovered and later used to prepare a stock colloidal solution with a loading of 1 g/L in titania in 0.01 M HCl aqueous media.

Extinction and absorption spectra, and determination of the fraction of photon flow absorbed by TiO_2

The extinction and absorption spectra at various titania loadings at pH ≈ 2 were recorded using a 0.2-mm quartz cell and a Shimadzu UV-265 spectrophotometer equipped with an integrating sphere (Fig. 2) with an internal diameter of 60 mm and a R-446 U photomultiplier at the base (incidence angle to reflecting sample: 8°; beam size ≈3 mm width and 5.5 mm height. The standard white reflecting plates contained $BaSO_4$ (Eastman Kodak White Reference Standard; reflectance, 98.23% at 365 nm). The modified method used to assess the fraction of the photon flow, $f_{\lambda,}$ absorbed by the titania solutions (loading range: 10 mg/L–150 mg/L) is identical to that reported earlier [18,19].

The method of calculating the absorption spectra with the integrating sphere followed the method of Sun & Bolton who used an identical instrument [18,19]. With the 0.20-mm cell and the geometry of the integrating sphere, unaccountable light scattered was negligible. Under our conditions, the instrument response A_1 for a solution with no titania particles is given by,

$$A_1 = \frac{-\lg(E_o - 2E_a)}{E_o} \tag{1}$$

whereas

$$A_2 = \frac{-\lg(E_o - 2E_a - 2E_a^{sol})}{E_o} \tag{2}$$

is the response for the titania colloidal solution from which the fraction f_λ was evaluated; E_o is the light irradiance from the light source and E_a is the irradiance of the light absorbed.

$$f_\lambda = \frac{10^{A_1} - 10^{A_2}}{2} \tag{3}$$

The absorbance spectrum of the titania particles in the solution was calculated from

$$A = -\lg(1 - f_\lambda) \tag{4}$$

The incident photon flow $R_{o,\lambda}$ at 365 ± 10 nm was determined by Aberchrome 540 actinometry [26].

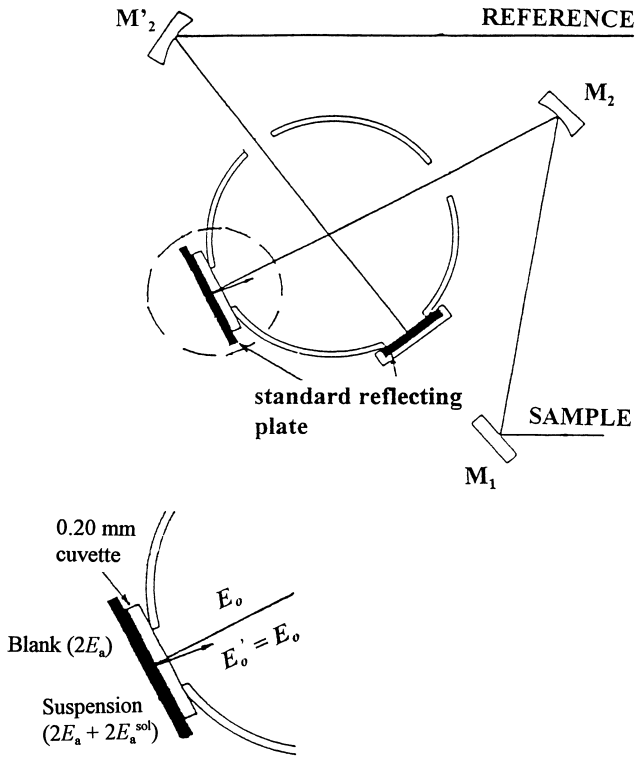

Fig. 2 Modified integrating sphere assembly method to determine the fraction of absorbed light for titania colloidal solutions.

Figure 3 summarizes the fraction of photon flow f_λ absorbed at 365 nm for the Degussa P-25 TiO_2 and the Hombikat UV-100 TiO_2 solution specimens in the concentration range 0.010–0.150 g/L. The fraction of light absorbed at loadings of 0.300 and 0.500 g/L were estimated assuming Beer's law behavior (see Table 1).

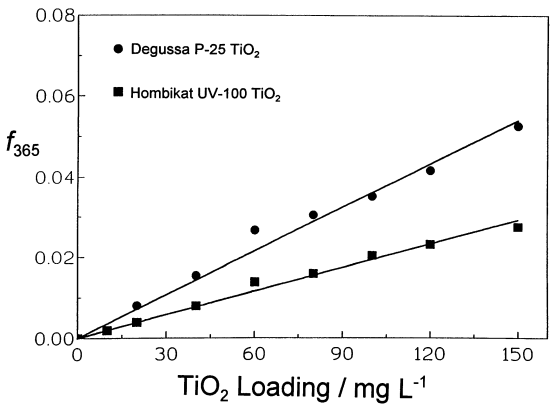

Fig. 3 Fraction of photon flow absorbed at 365 nm vs. titania solution concentration for the Degussa P-25 TiO_2 and the Hombikat UV-100 TiO_2 specimens.

Determination of quantum yields

In the photocatalyzed oxidations of phenol and 4-chlorophenol by illuminated titania particulates, as indicated in Part I [14], the titania/phenol aqueous dispersion was stirred in the dark for about 30–60 min to bring the system to an adsorption/desorption equilibrium stage prior to irradiation.

Table 1 Initial rates, R^{in}, photon flow, $R_{o,\lambda}$, fraction of light absorbed at 365 nm, f_{365}, quantum yields for the initial photocatalyzed oxidative transformation of phenol, Φ_{dis} (PhOH), and photonic efficiencies, ξ, at ambient temperature and for air-equilibrated solutions

TiO_2 loading (g/L)	$10^8\ R^{in}$ (mol/min)	$10^6\ R_{o,365}$* (einstein/min)	f_{365}†	Φ_{dis} (PhOH)	$10^3\ \xi_{365}$§
0.060	0.54 ± 0.21	2.13	0.0216	0.118	2.5 ± 1.0
0.10	1.31 ± 0.65	2.60	0.0359	0.140	5.0 ± 2.5
0.15	1.91 ± 0.61	2.13	0.0539	0.167	9.0 ± 2.9
0.30	3.14 ± 1.02	2.13	(0.108)‡	0.137	14.7 ± 4.8
0.50	5.00 ± 0.26	2.13	(0.180)‡	0.131	23.5 ± 1.2
1.0	4.49 ± 0.51	1.86	–	–	24.1 ± 2.4
1.0	5.13 ± 0.45	2.05	–	–	25.0 ± 2.1
2.0	6.08 ± 0.72	1.69	–	–	35.9 ± 3.4
3.0	6.27 ± 0.79	1.69	–	–	37.0 ± 3.7
4.0	6.33 ± 0.75	1.69	–	–	37.5 ± 3.5
				Average Φ_{dis} (PhOH) = 0.14 ± 0.02	

* The incident photon flow was measured by Aberchrome actinometry using a procedure supplied by Aberchromics Ltd. of the University of Wales College of Cardiff, Cardiff CF1 3TB, UK.
† Corrected (see Fig. 9).
‡ Estimated from the experimentally obtained fraction of light absorbed for TiO_2 loadings from 10 mg/L to 150 mg/L. (See Fig. 3).
§ Calculated from equation $\xi_{365} = R^{in}/R_{o,365}$.

The initial rates of the photocatalyzed oxidation of phenol (Aldrich, 99% + redistilled; pH was 2.7) were obtained by monitoring the temporal variations of the concentration of phenol by HPLC chromatography (Waters 501 HPLC pump; Waters 441 HPLC detector; HP 3396A integrator; Waters Bondapak C-18 reverse phase column) after 365 ± 10 nm irradiation (selected with Bausch & Lomb 0.25-meter monochromator) of the aqueous TiO_2/phenol dispersion in a quartz reactor employing an Oriel 1000-watt Hg/Xe lamp as the radiation source. Samples were collected at various time intervals and filtered through a 0.20-μm Teflon filter prior to HPLC analysis to remove suspended particulates. Initial rate data are given in Table 1 and illustrated in Fig. 4.

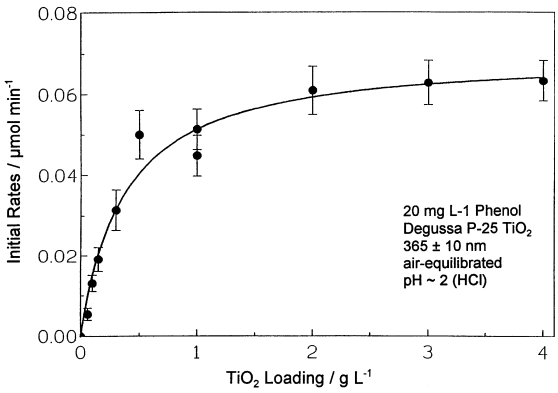

Fig. 4 Initial rates for the photooxidative degradation of phenol vs. TiO_2 loading for the Degussa P-25 TiO_2 specimen.

RESULTS AND DISCUSSION

In Part I [14] we observed that when a photon hits a photocatalyst particle such as TiO_2 in condensed phase, the fraction of light scattered (E_{sc}/E_o) depends on several factors: (i) on the number of particles

(N_p), (ii) on the square of the particle volume (V^2)—hence on the sixth power of the particle radius, (iii) on a geometric factor {$P(\theta)$} that accounts for scattering from different parts of the particle, (iv) on the reciprocal of the fourth power of the wavelength of irradiation (λ^{-4}), and (v) on the square of the distance of the observer (detector), r^2, from the particle. A more crucial factor that affects E_{sc}/E_o is the fourth power of the ratio of the refractive indices {$(n_1/n_o)^4$} of the photocatalyst particle (n_1) and of the surrounding medium (n_o).

For the particular case examined here, two variables are most critical to the fractional light scattering: an increase in the TiO_2 loading {N_p} increases scattering and increasing the size (radius, R) of either the particles (~30-nm crystallites) or of the ubiquitous particle aggregates, usually omnipresent in such suspensions, augments scattering significantly since $E_{sc}/E_o \propto R^6$.

Extinction and absorption spectra

Extinction (i.e. absorption and scattering/reflection of light by a substrate) and absorption spectra of TiO_2 dispersions were recorded at low titania loadings by normal absorption spectroscopy and by an integrated sphere method, respectively, to explore the extent of light scattered by nanoparticles. This method contrasts the one proposed recently by Grela *et al*. [20]. Determination of the degree of scattering in titania dispersions is especially critical since TiO_2 has even been suggested as an actinometer for UV radiation [27].

Figure 5 illustrates the extinction spectra of the Degussa P-25 TiO_2 and the Hombikat UV-100 TiO_2 in aqueous phase. Also shown are the scattering curves extrapolated to the ultraviolet range from the experimental baseline in the visible region using the quadratic polynomial expression (eqn 5) to probe the extent of light scattered in the UV region [20],

$$E_{sc} = a + b\lambda + c\lambda^2 \quad (5)$$

where TiO_2 absorbs significantly (a, b and c are coefficients).

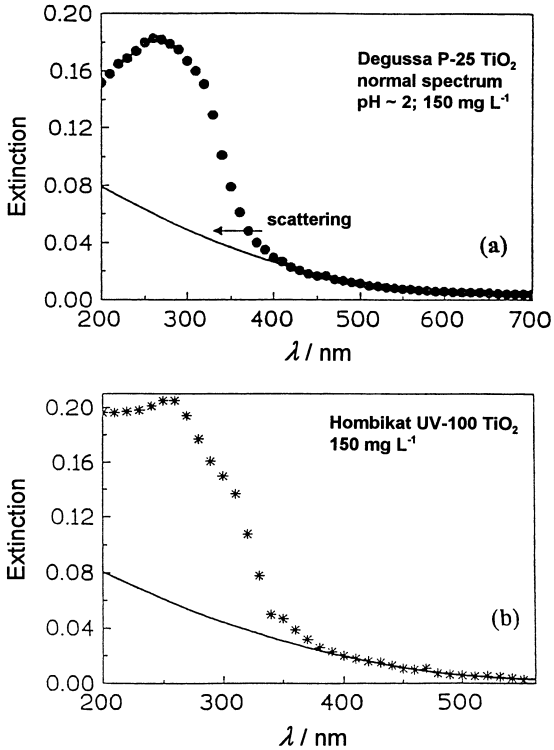

Fig. 5 Extinction spectra (solid circles and asterisks) of polydispersed TiO_2 solutions in aqueous media at pH ≈ 2; loading, 150 mg/L. (a) Degussa P-25 TiO_2; (b) Hombikat UV-100 TiO_2. The solid line that extrapolates the baseline from the visible region reflects the scattering of light; the extrapolation was carried out by a quadratic polynomial (see text).

The extinction spectra of titania solutions at 40 mg/L and 150 mg/L loading are compared with the calculated (integrating sphere) absorbance spectra (Fig. 6) by the method reported earlier [18,19].

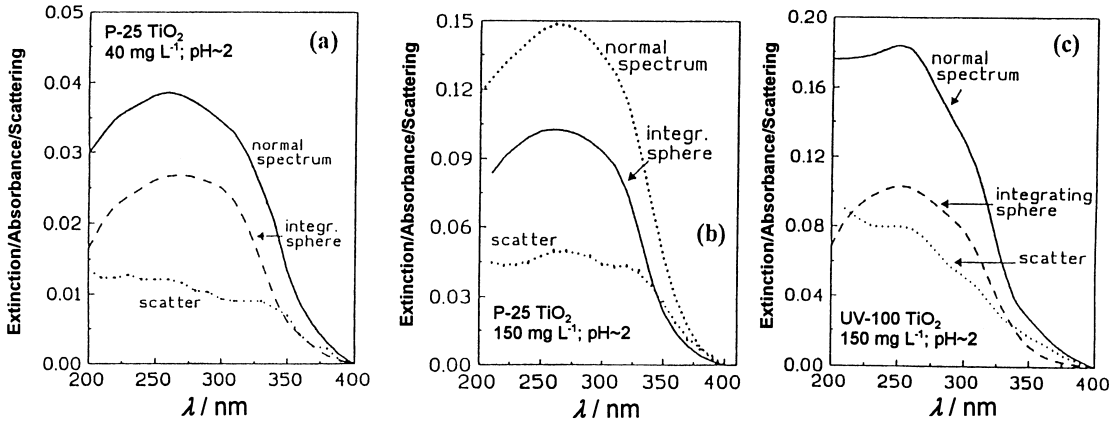

Fig. 6 Plots illustrating the extinction (normal spectrum), absorbance (integrating sphere method) and scattering (obtained by subtracting the absorbance from the extinction spectra) of polydispersed titania solutions: (a) 40 mg/L Degussa P-25 TiO_2; (b) 150 mg/L Degussa P-25 TiO_2; (c) 150 mg/L Hombikat UV-100 TiO_2. All spectra were corrected for the extent of scattering in the visible region and thus placed at zero at 400 nm.

The differences between the extinction spectra and the absorbance spectra are also illustrated; they reflect the wavelength-dependent scattering component in the extinction spectra. In the comparison, the values were set to zero at 400 nm where anatase titania does not absorb. (Note that the absorption threshold of titania anatase used is at ≈385 nm.) The scattering component increases monotonically up to ≈350 nm and then levels off to 200 nm for the Degussa P-25 TiO_2 (~80% anatase). For the Hombikat UV-100 TiO_2 anatase specimen [25], the scattering component increases continually from 400 nm to 200 nm. Evidently, scattering is greatly attenuated as titania absorption increases in the UV region, as expected. Indeed, relative scattering drops from ≈80% at 390 nm to about 30–40% at 300 nm for the 150 mg/L Degussa P-25 TiO_2 and to ≈40–50% at 320 nm for the corresponding Hombikat UV-100 titania sample. However, to the extent that the degree of light absorption can be as low as ≈15% [15,16], the (apparent) quantum yields determined by the extrapolation method [20] could be discrepant by as much as a factor of 2–5.

More revealing are the comparisons between the experimental (at wavelengths >400 nm) and the quadratic and cubic polynomial extrapolations (to wavelengths <400 nm) of the light scattering components illustrated in Fig. 7a,b for the 40 mg/L and 150 mg/L Degussa P-25 TiO_2 loading, respectively, and for the Hombikat UV-100 TiO_2 sample (also 150 mg/L; Fig. 7c). The scattering components in Fig. 6 were added to the corresponding experimental scattering (data points) in Fig. 7. It is clear that the quadratic extrapolation method (curves b in Fig. 7) [20] significantly underestimates the experimental scattering component (curves a) between 380 nm and 220 nm in two cases presented (Figs 7a,b), whereas for the Hombikat UV-100 TiO_2 specimen (Fig. 7c) this extrapolation totally underestimates the scattering component at allwavelengths below 380 nm. The cubic extrapolation (curves c in Fig. 7a,b,c; here the term $d\lambda^3$ was added to eqn 5) is an improvement but still underestimates the scattering behavior of the titania solutions.

The scattering component does indeed follow the expected λ^{-4} dependence as demonstrated in Fig. 8a for the Degussa P-25 TiO_2 for all wavelengths down to 350 nm, and in Fig. 8b for the Hombikat UV-100 TiO_2 system down to 250 nm. At shorter wavelengths, the scattering levels off in both instances (see caption in Fig. 8).

It is clear that the empirical method used [20] to assess the degree of scattering consistently underestimates the extent of scattering below 380 nm. Scattering tends to plateau for the Degussa P-25 TiO_2 solutions (not for the Hombikat UV-100 TiO_2 specimen) below ≈340 nm in the region where they absorb significantly.

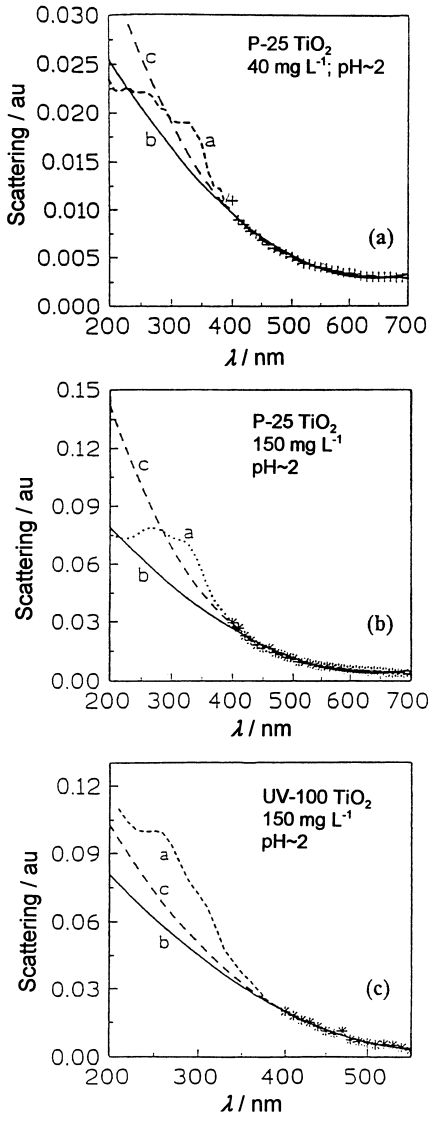

Fig. 7 Plots showing the experimental base line at wavelengths above 400 nm (scattering) for the three titania samples at different loadings (see Fig. 6). The curve a in each graph denotes the scattering component in the 200–400 nm region (see Fig. 6) added to the visible component. Curve b refers to the scattering expected from the extrapolation using the quadratic polynomial method, whereas curve c is the scattering component expected if we use a cubic polynomial method (see text).

The spectral features of Fig. 6 are qualitatively similar to the features reported recently by Cabrera and co-workers [28] for TiO_2 specimens from various sources (Degussa P-25 TiO_2, Hombikat UV-100 TiO_2, Fluka, Fisher, Aldrich and Merck). These authors also assessed the specific extinction (Fig. 9A), scattering (Fig. 9B), and absorption (Fig. 9C) coefficients in the UV region (270–400 nm) illustrated here only for the Degussa P-25 TiO_2 and Hombikat UV-100 TiO_2 systems. Figure 9D illustrates the scattering vs. absorption ratio at various wavelengths; note the relatively rapid rise in scattering towards the visible wavelengths. Except for the Degussa P-25 TiO_2 and the Hombikat UV-100 TiO_2 specimens, the specific absorption coefficients for all other samples are fairly similar and constant. At 360–370 nm the specific absorption coefficients for the Degussa P-25 and Hombikat UV-100 TiO_2 are less than that for the other titania specimens. The specific scattering coefficients follow the trend: Fisher/Fluka < Hombikat UV-100 < Merck < Aldrich << Degussa P-25. Scattering influences the extinction spectra which follow a

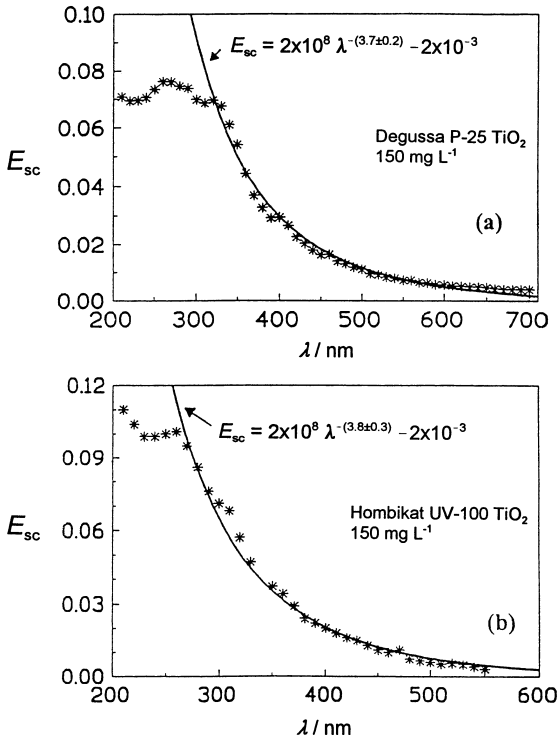

Fig. 8 Scattering for the Degussa P-25 TiO_2 (a) and the Hombikat UV-100 TiO_2 (b), at 150 mg/L loading. The solid curve in both graphs drawn using the equation indicated, namely scattering follows the λ^{-4} law down to $\approx$ 340 nm for Degussa P-25 TiO_2 and to $\approx$ 260 nm for the Hombikat UV-100 TiO_2 specimen. The apparent levelling off at the shorter wavelengths is due to the considerable attenuation of the scattering by the increased absorption in this region of the UV.

similar trend. On the basis of specific surface area alone, the authors [28] inferred that the catalytic properties should follow the trend: Hombikat UV-100 >>> Degussa P-25 >> Aldrich/Merck/Fluka/Fisher. However, taking into account the photonic properties of these specimens, the expected process photonic efficiencies should be: Degussa P-25 >>> Aldrich/Merck/Fluka/Fisher > Hombikat UV-100 [28]. This trend is consistent with the photonic efficiencies we observed earlier [17,25] between the Degussa P-25 and the Hombikat UV-100 TiO_2 specimens.

We deduce from our spectroscopic data that any determination of *absolute* quantum yields in heterogeneous photochemistry necessitates an experimental approach to assess the number (or photon flow) of absorbed photons; the integrating sphere method is one such approach since the transmitted, scattered and absorbed photons can be accounted for. Quadratic or cubic polynomial extrapolations of the spectral baseline in the visible region remain simply approximations that if used will still only provide an *apparent* quantum yield [20] for the process being examined.

Determination of quantum yields

Perusal of the initial rates of photodegradation of phenol (Table 1) by illuminated Degussa P-25 TiO_2 together with the corresponding graphical representation of R^{in} as a function of increasing TiO_2 loading (Fig. 4) shows that the rates increase linearly from 0 to 0.50 g/L loading and then level off to 4.0 g/L loading. This is understandable since, as the titania loading increases, the suspension becomes more opaque to light such that only photons absorbed by titania particles onto which a phenol molecule is preadsorbed may be effective in carrying out the redox chemistry. Other incident photons, absorbed or otherwise, are wasted. In essence the titania particles themselves act as an inner filter (see Fig. 10) despite good stirring of the dispersion during irradiation, a problem also encountered in homogeneous photochemistry.

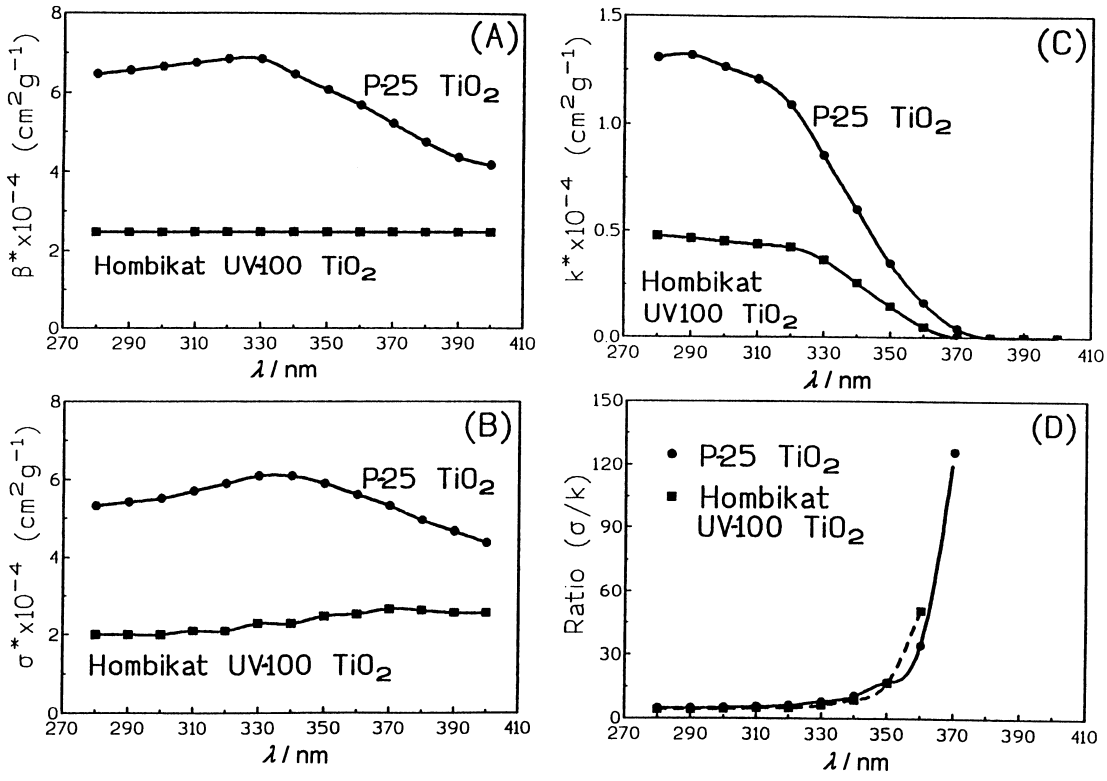

Fig. 9 (a) Extinction coefficients vs. wavelength for Degussa P-25 TiO_2 and for Hombikat UV-100 TiO_2 particles; (b) scattering coefficients of the Degussa P-25 TiO_2 and the Hombikat UV-100 TiO_2 particles; (c) absorption coefficients of the Degussa P-25 TiO_2 and Hombikat UV-100 TiO_2 particles; (d) scattering to absorption coefficients ratio of the Degussa P-25 TiO_2 and Hombikat UV-100 TiO_2 particles. Data adapted from [28].

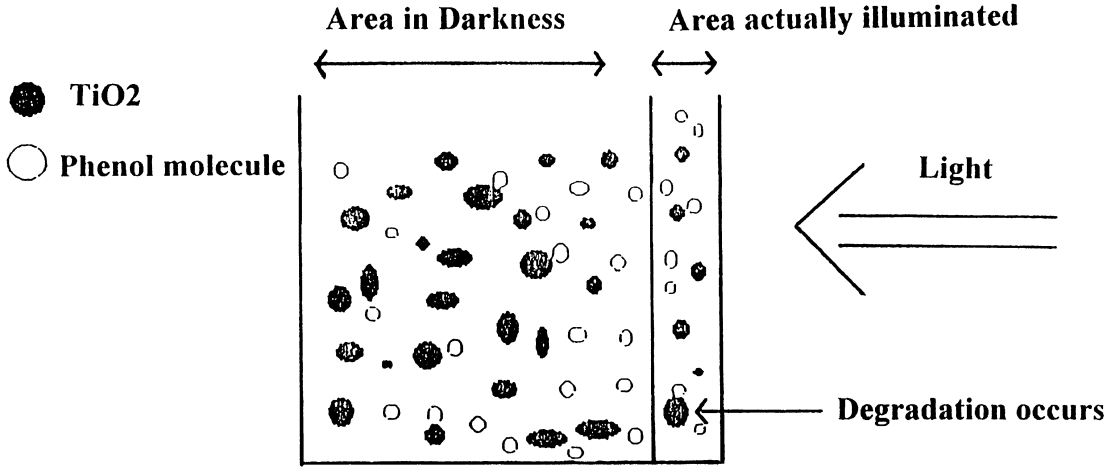

Fig. 10 Typical reactor cell used in the photocatalyzed oxidative degradation of phenol in determining initial rates of disappearance of phenol and subsequently the preliminary quantum yield data.

Given the fraction of light absorbed at 365 nm, f_{365} in Table 1, together with the initial rates of photooxidation of phenol, R^{in}, under 365 nm irradiation and with the rate of incident photons, $R_{o,\lambda}$, at TiO_2 loadings from 0.060 to 0.500 g/L collected in Table 1 we calculated the quantum yield by eqn 6:

$$\Phi_{phenol} = \frac{R^{in}}{R_{o,365}\, f_{365}} \tag{6}$$

The resulting quantum yields are summarized in Table 1 for five titania loadings for which initial rates are nearly linear with loading. The average Φ_{phenol} (365 nm) for the initial photodegradation of phenol is 0.14 ± 0.02. The photonic efficiency dependence on the TiO_2 loading reported in table 1 and shown graphically in fig. 2 of Part I [14] follow the expected Langmuirian type trend. The intercept from the linear transform gave a limiting photonic efficiency of $\xi_{lim} \approx 0.12$, in good agreement with the estimated quantum yield (Table 1).

In an independent set of experiments, we determined the photonic efficiencies (as $\xi = R^{in}/R_{o,300-400}$) for the photooxidation of 20 mg/L phenol with irradiated Degussa P-25 TiO_2 (0.050–4.0 g/L loading) under broadband radiation ($\approx$ 300–400 nm) at pH $\approx$ 2 in a pyrex reactor (Fig. 11). The insert in Fig. 11 illustrates the corresponding linear transform of the data. The limiting photonic efficiency, ξ_{lim}, at high titania loading is surprisingly also 0.14 ± 0.01. In this instance, the Degussa P-25 TiO_2 specimen received no prior treatment, except for allowance made to stir the dispersion to establish the adsorption/desorption equilibrium.

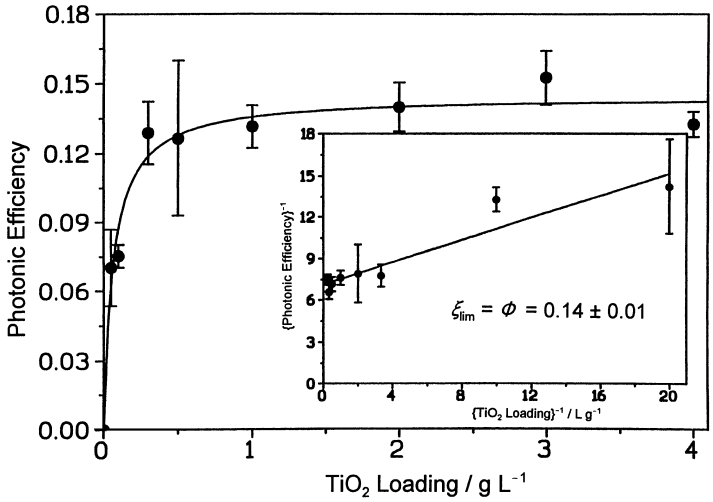

Fig. 11 Photonic efficiencies vs. TiO_2 loading (Degussa P-25) for the photodegradation of phenol (20 mg/L) in air-equilibrated suspensions at pH $\approx$ 2 (HCl); wavelength range of irradiation: 300–400 nm. The Degussa P-25 TiO_2 was used without any prior treatment.

The quantum yields for the photooxidation of other organic substrates and of phenol using other photocatalyst materials (tables 1 and 2 of [14]), experiments done under otherwise identical conditions, were reported earlier. The validity of the procedure advocated herein was further assessed by determining first the photonic efficiencies and subsequently from the limiting photonic efficiency the quantum yield for the photooxidation of 4-chlorophenol: $\xi_{lim} = \Phi = 0.19 \pm 0.02$, in good agreement with the estimated value of 0.17 ± 0.02 [14]. Likewise, we assessed the limiting photonic efficiency for the photooxidation of phenol using the Hombikat UV-100 TiO_2 under conditions otherwise similar to those employed for the Degussa P-25 TiO_2 system (loading 0.10–5.0 g/L, pyrex reactor, pH $\approx$ 2, broadband radiation from 300 nm to 400 nm). The ξ_{lim} was 0.052 ± 0.009, a value consistent with the estimated quantum yield of 0.035 ± 0.003 (table 2 of [14]).

CONCLUDING REMARKS

In Part I we presented a useful protocol, *Relative Photonic Efficiency*, ξ_r, to correlate efficiencies of a given process in a heterogeneous (solid/gas or solid/liquid) photocatalytic experiment with similar work from other laboratories. The procedure is simple and required no sophisticated instrumentation. ξ_r is convertible to ***quantum yields*** for the photocatalyzed oxidation of a given substrate since the quantum yield for the photooxidative degradation of phenol, Φ_{phenol}, was assessed by first determining the fraction of the incident photon flow from the radiation source absorbed by the photocatalyst material Degussa

P-25 TiO_2 taken as a standard using a spectrophotometric integrating sphere method. Quantum yields so calculated from relative photonic efficiencies satisfied the photochemical definition of Φ of homogeneous photochemistry. In this Part II article we have presented some of the issues regarding the noninsignificant extent of light scattered by the heterogeneous phase and have also dealt with a potentially useful experimental method to determine the process quantum yield by assessing the limiting relative photonic efficiency ξ_{lim} that is equivalent to Φ when complete absorption of light takes place at high photocatalyst loadings.

From the few cases so far examined, the method of limiting photonic efficiencies to ascertain an estimate of the true quantum yield is worth pursuing, with due care for the precision in the experimental data as this extrapolation method (see insert to Fig. 11) carries substantial uncertainty. Currently, the factors that affect the quantum yields of photochemical processes on the surface of nano/microparticulates of wide bandgap metal oxides in solid/gas and solid/liquid heterogeneous systems are being examined theoretically [29] by solving the continuity equation for a one-dimensional plate, and by considering also the spatial nonuniformity of photogeneration of charge carriers in the bulk of the solids and their limited probability of diffusion toward the particle surface.

ACKNOWLEDGEMENTS

Financial support of this work by the Natural Sciences and Engineering Research Council of Canada (no. A5443 to N.S.), by the National Natural Science Foundation of China (no. 29677019 and no. 29725715 to J.Z.) and by Grants-in-aid for Scientific Research from the Japanese Ministry of Education (no. 10640569 to H.H.) is gratefully acknowledged. We also thank Mr J. van de Ven for some of the preliminary experiments and Dr L. Cai for technical assistance. We have also benefited much from the useful comments and discussions we have had with Prof. J. R. Bolton (University of Western Ontario, Canada) and Dr P. V. Kamat (Radiation Laboratory, University of Notre Dame).

REFERENCES

1 N. Serpone. In *Kirk-Othmer Encyclopedia of Chemical Technology*, Vol. 18, pp. 820–837. Wiley-Interscience, New York (1996).

2 M. A. Fox, M. T. Dulay. *Chem. Rev.* **93**, 341 (1993).

3 P. V. Kamat. *Chem. Rev.* **93**, 267 (1993).

4 A. Heller. *Acc. Chem. Res.* **28**, 503 (1995).

5 M. R. Hoffmann, S. T. Martin, W. Choi, D. F. Bahnemann. *Chem. Rev.* **95**, 69 (1995).

6 D. F. Bahnemann, J. Cunningham, M. A. Fox, E. Pelizzetti, P. Pichat, N. Serpone. In *Aquatic and Surface Photochemistry* (D. Crosby, G. Helz, R. Zepp, eds), pp. 261–316. Lewis Publishers, Boca Raton, FL (1994).

7 D. F. Ollis, H. Al-Ekabi, eds. *Photocatalytic Purification and Treatment of Water and Air*. Elsevier Science, Amsterdam (1993).

8 N. Serpone, E. Pelizzetti. *Photocatalysis—Fundamentals and Applications*. Wiley-Interscience, New York (1989).

9 N. Serpone. *Res. Chem. Interm.* **20**, 953 (1994).

10 M. K. Nazeeruddin, K. Kay, I. Rodicio, R. Humphry-Baker, E. Mueller, N. Vlachopoulos, M. Gratzel. *J. Am. Chem. Soc.* **115**, 6382 (1993).

11 (a) N. Serpone, D. Lawless, R. F. Khairutdinov, E. Pelizzetti. *J. Phys. Chem.* **99**, 16 655 (1995). (b) N. Serpone, D. Lawless, R.F. Khairutdinov. *J. Phys. Chem.* **99**, 16 646 (1995).

12 (a) J. Zhao, H. Hidaka, A. Takamura, E. Pelizzetti, N. Serpone. *Langmuir*, **9**, 1646 (1993). (b) H. Hidaka, Y. Suzuki, K. Nohara, S. Horikoshi, Y. Hisamatsu, E. Pelizzetti, N. Serpone. *J. Polym. Sci. A. Polym. Chem.* **34**, 1311 (1996).

13 N. Serpone, E. Pelizzetti, H. Hidaka. In *Photochemical and Photoelectrochemical Conversion and Storage of Solar Energy* (Z. W. Tian, Y. Cao, eds.), pp. 33–73. International Academic Publishers, Beijing, China (1993).

14 IUPAC Commission on Photochemistry (N. Serpone, A. Salinaro). Terminology, relative phototonic efficiency and quantum yields in heterogeneous photocatalysis. Part I: Suggested protocol (Technical Report). *Pure Appl. Chem.* **71**, 303–320 (1999).

15 V. Augugliaro, V. Loddo, L. Palmisano, M. Schiavello. *Sol. Energy Mater. Sol. Cells* **38**, 411 (1995).

16 M. I. Cabrera, O. M. Alfano, A. E. Cassano. *Ind. Eng. Chem. Res.* **33**, 3031 (1994).

17 N. Serpone, G. Sauve, R. Koch, H. Tahiri, P. Pichat, P. Piccinini, E. Pelizzetti, H. Hidaka. *J. Photochem. Photobiol. A. Chem.* **94**, 191 (1996).

18 L. Sun, J. R. Bolton. *J. Phys. Chem.* **99**, 4127 (1995).

19 N. Serpone. *J. Photochem. Photobiol. A. Chem.* **104**, 1 (1997).

20 M. A. Grela, M. E. J. Coronel, A. J. Colussi. *J. Phys. Chem.* **100**, 16940 (1996).

21 G. Riegel, J. R. Bolton. *J. Phys. Chem.* **99**, 4215 (1995).

22 K. Tanaka, M. F. V. Capule, T. Hisanaga. *Chem. Phys. Lett.* **187**, 73 (1991).

23 P. Ruterana, P.-A. Buffat, K. R. Thampi, M. Gratzel. *Mater. Res. Soc. Symp. Proc.* **139**, 327 (1989).

24 P. Ruterana, P.-A. Buffat, K. R. Thampi, M. Gratzel. *Ultramicroscopy* **34**, 66 (1990).

25 H. Tahiri, N. Serpone, R. Le van Mao. *J. Photochem. Photobiol. A. Chem.* **93**, 199 (1996).

26 H. G. Heller, J. R. Langman. *J. Chem. Soc. Perkin II* 341 (1981); see also information bulletin from Aberchromics Ltd, The University of Wales, College of Cardiff, Cardiff CF1 3TB, UK.

27 C. Huang, *et al*. *Anal. Chim. Acta* **311**, 115 (1995).

28 M. I. Cabrera, O. M. Alfano, A. E. Cassano. *J. Phys. Chem.* **100**, 20 043 (1996).

29 A. V. Emeline, V. K. Ryabchuk, N. Serpone. *J. Phys. Chem. B* **103**, 1316 (1999).